Int. J. Electrochem. Sci., 17 **(2022)** Article Number: 220227, doi: 10.20964/2022.02.14

International Journal of
ELECTROCHEMICAL
SCIENCE
www.electrochemsci.org

Mini review

Application of Hybridization Chain Reaction (HCR) in Electrochemical Analysis

Qiongyu Zhang

School of Fundamental Sciences, Yongzhou Vocational Technical College, Yongzhou 425100, Hunan, China
E-mail: qiongyuzhang2009@163.com

Received: 1 November 2021 / *Accepted:* 29 November 2021 / *Published:* 5 January 2022

With the bloom of DNA nanotechnology, diverse DNA amplification strategies have been designed and applied in bioassays. Among them, hybridization chain reaction (HCR) is prevalent because of its advantages of simplicity, enzyme-free and isothermal amplification. HCR-based electrochemical biosensors have been widely used in broad fields of food safety, environmental monitor and disease diagnosis. This review highlights the progress in HCR-based electrochemical biosensors which are divided based on the types of signal reporters.

Keywords: Hybridization chain reaction; electrochemical biosensor; nanomaterials; signal amplification

1. INTRODUCTION

During the past several decades, the exponentially development of varied nucleic acid amplification technologies has attracted increasing attention in the biosensing-related fields [1]. These amplification technologies can be classified into two different groups: thermal cycle amplification technology and isothermal amplification technology [2, 3]. The former includes polymerase chain reaction (PCR), ligase chain reaction (LCR), nucleic acid sequence amplification (NASA) and so on. The latter contains helix-related amplification (HDA), rolling loop amplification (RCA), and catalytic hairpin assembly (CHA), etc. Although the PCR technology is widely employed to detect nucleic acids in laboratories and hospitals, it always requires complex operation process and strict heating/cooling cycle procedures. Moreover, the use of enzymes may limit the real application of RCA.

Since being first reported by Dirks and Pierce in 2004, hybridization chain reaction (HCR) has becoming a vital and powerful DNA-based signal amplification technique for chemical and biological

sensing [4-6]. It is a simple, isothermal, enzyme-free reaction process. Briefly, a typical HCR system involves an initiator and two metastable complementary DNA hairpins (H1 and H2). The initiator can open H1 and the unfolded H1 then triggers the opening of H2. Consequently, a cascade reaction happens to form a long-nicked DNA polymer. In the absence of the initiator, H1 and H2 are inactive of hybridization due to the energy barrier. Therefore, HCR-based method can effectively reduce the positive signal and the background signal owing to its initiator-response property. Moreover, HCR technique is recognized as an effective alternative strategy to PCR, because one copy of the initiator can trigger a cascade chain-growth polymerization of hairpins into a long polymer for generating significantly amplified signal.

Electrochemical approaches with HCR as the signal amplifier have already attracted more and more attention in bioassays due to their excellent sensitivity as low as the attomolar level [7-9]. At first, HCR is explored for the detection of nucleic acids that have been regarded as biomarkers and therapeutic targets for disease diagnosis. Benefiting to the contemporary advancement of aptamer technology, HCR has been further utilized as a versatile tool to sensitively detect other targets by molecular conversion, such as toxic metal ions, small metabolites, protein, enzyme activity and cells [10-13]. More importantly, through coupling antibodies with DNA initiator with bonds or NPs, one could convert the immunoreaction event into the HCR-based DNA amplification strategy [14-18]. For example, in the biobarcode assay, nanoparticles (NPs) are employed to carry DNA and antibody at a high ratio. After the immunoreaction, numerous DNA probes on NPs can be detected existing DNA-based amplification techniques. In proximity ligation assay (PLA), antibodies modified with DNA probes capture the same target and induce DNA assemblies [19, 20].

Furthermore, to realize target recycling, other DNA amplification techniques, such as catalyzed hairpin assembly reaction (CHA), nuclease (exonuclease/endonuclease)-assisted target recycling and strand-displacement amplification (SDA) have been combined with HCR into cascade signal amplification strategy for sensitive detection [21-24]. For instance, Wang et al. combined selective Ag^{+}-aided ligation with SDA and HCR for the detection of N^{6}-methyladenosine [25]. Zhu et al. reported the label-free electrochemical sensing of DNA by coupling the isothermal strand-displacement polymerase reaction with HCR for one-target-multi-triggers [26]. Despite simplicity, traditional linear HCR exhibits a relatively lower efficiency of hybridization and signal amplification. Thus, in recent years, with the emerging of diverse programming self-assembly methods, nonlinear HCR reactions have attracted extensive interest because of their higher amplification efficiency and ultrahigh sensitivity [27-30]. For example, Liu et al. fabricated a dendritic DNA concatamer by introducing three auxiliary DNA probes as HCR units for the detection of DNA and adenosine triphosphate [31]. Jiang et al. used dumbbell HCR system to develop an aptasensor for prostate specific antigen detection [32].

In this review, the development of HCR-based electrochemical method for chemical and biological sensing was summarized. The works are classified according to the type of signal reporters, including redox molecules, natural enzyme, DNAzyme and nanomaterials. Moreover, three important types of works were also summarized, including immobilization-free, magnetic or nanoparticles-based, and ratiometric methods.

2. HCR-BASED ELECTROCHEMICAL METHODS

Generally, there are two ways to label DNA probes or DNA concatemers. One of them is to conjugate the probe with electroactive species (such as redox molecules and nanomaterials) or catalytic elements (such as enzyme, enzyme mimics and nanocatalysts). The other one is to use HCR products (DNA nanowires) as the carriers or templates for the assembly of electroactive species or nanomaterials via non-covalent interactions without the use of labels in advance.

2.1 Redox molecules

In an electrochemical method, redox molecules are necessary to exchange electrons with the electrode and generate the current or impedance, no matter they are conjugated with or intercalated into biological recognition elements. Up to now, many redox species have already been employed in electrochemistry-related assays, such as $[Ru(NH_3)_6]^{3+}$ (RuHex), methylene blue (MetB) and ferrocene (Fc) [33]. Nowadays, it is a usual way to label hairpin-shaped signal probes with redox molecules for signal output [34-36]. Moreover, the multiple assays can be realized by using distinguishable electrochemical signal molecules as the redox labels [37, 38]. For example, Ren et al. labeled two hairpin probes with MetB for "signal-on" electrochemical detection of DNA by Exo III and HCR amplification [39]. Jiang et al. reported a cheap and sensitive electrochemical cloth-based DNA biosensor through double linear HCR (DL-HCR) [40]. As presented in Figure 1A, the nanocomposites of CdTe quantum dots and multiwalled carbon nanotubes were employed to modify the cloth-based sensing interface. DL-HCR generated from Fc-labeled DNA probes could significantly amplify the electrochemical signal. Recently, it has attracted much attention to integrate proximity ligation or hybridization assays with HCR for biomolecular detection [41]. Liu et al. presented a novel proof-of-principle of dynamic DNA assembly-programmed surface hybridization that could be coupled with diverse homogeneous target recognition and HCR amplification [42]. As shown in Figure 1B, although the short tail in solo DNA hairpin was complementary to the surface-immobilized DNA, the predesigned low melting temperature (< 37 ^{o}C) could not afford to fix hairpin on the electrode. However, after the HCR reaction, abundant tail sequences in DNA polymers were bound to the surface because their local concentration is enough high for their hybridization with the surface-tethered capture probes. The specific complex of biotin and streptavidin (SA) can also be employed to label DNA concatamer from HCR. For example, Zhu et al. reported a sandwich-type electrochemical immunosensor for four biomarkers based on HCR and biotin-SA signal amplification [38]. In this study, after the immunoreaction, biotin-labeled detection antibody was derived with SA and biotin-labeled DNA initiator to trigger HCR. Then, the formed biotin-functionalized DNA concatamer was further derived with redox-labeled SA.

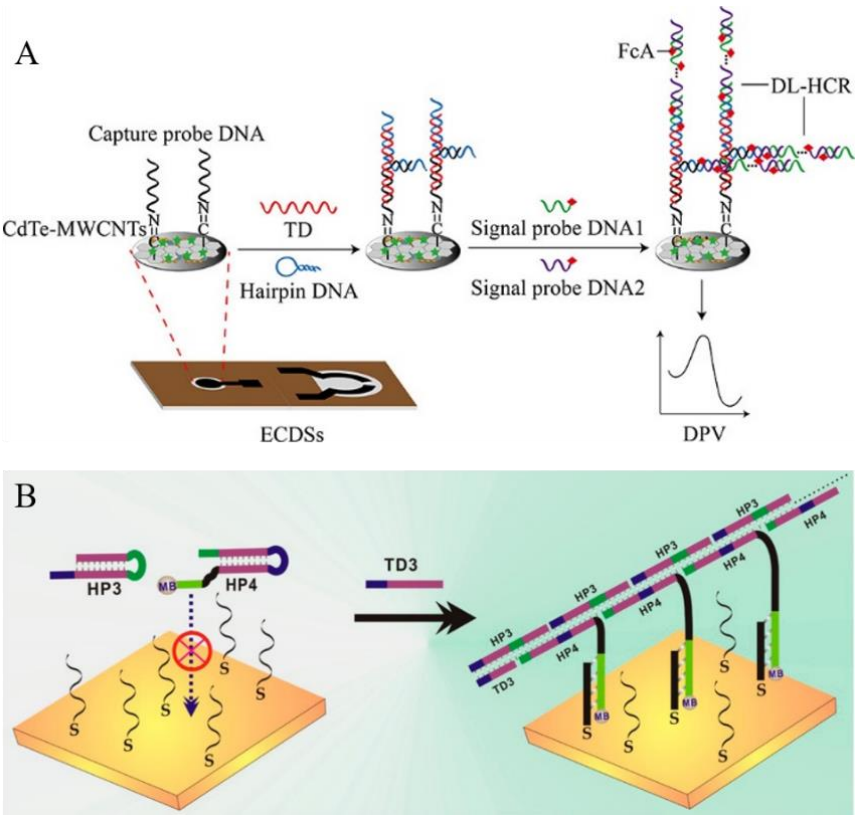

Figure 1. (**A**) Schematic illustration of the unfolded cloth-based device and preparation and detection processes of electrochemical cloth-based DNA biosensor [40]. Copyright 2020 American Chemical Society. (**B**) Schematic illustration for the HCR-programmed surface hybridization strategy [42]. Copyright 2017 American Chemical Society.

HCR product dsDNA ploymers with groove and phosphate moieties can bind redox molecules or complexes via electrostatic interaction or intercalation in a stoichiometric approach, which directly reflects the amounts of dsDNA on the electrode [43-45]. Yang et al. reported a label-free electrochemical genesensor by using RuHex to interact with HCR product [46]. Zeng et al. developed a label-free aptasensor of kanamycin by coupling SDA and HCR by using MetB as the indicator [47]. Guo et al. reported an enzyme-free HCR-based multiple immunosensor by using doxorubicin hydrochloride (DXH) and MetB as the intercalated molecules [48]. The density and orientation of DNA hairpin on the electrode surface have an important influence on the efficiency of HCR and detection performances. To well control these factors, Guo et al. demonstrated that mixing DNA hairpin with short straight ssDNA on the electrode could guarantee a sufficient distance between the probes [49]. As shown in Figure 2A, before the detection of miR-122, exonuclease I (Exo I) was added to cleave curly ssDNA hairpin to eliminate the false positive signal and decrease the background signal. In the presence of exosomal microRNA-122, long DNA polymers from HCR could capture more RuHex and generate an enhanced differential pulse voltammetry (DPV) signal. $Ru(phen)_3^{2+}$ is a highly efficient ECL luminescent reagent and can be inserted into the dsDNA groove. Chen et al. reported an universal electrochemiluminescent (ECL) method for the detection of DNA based in situ HCR amplification [50]. As illustrated in Figure 2B, target DNA from *Escherichia coli* uropathogen resulted in the generation of DNA polymers through the in situ HCR reaction. Then, a large amount of $Ru(phen)_3^{2+}$ ions were embeded into dsDNA helix and

produced a high ECL signal. This sensitive and universal HCR-based ECL method could be applied to analyze different biomolecules. Huang et al. proposed a proximity hybridization-triggered HCR (proxHCR) strategy for ECL detection of nuclear factor kappa B p50 [51]. In this work, proximity hybridization assay (PHA) was introduced to conversing protein detection to DNA detection. Target protein could protect 5'P-dsDNA from hydrolysis by λ exonuclease and 5'P-dsDNA acted as a trigger to initiate the HCR reaction.

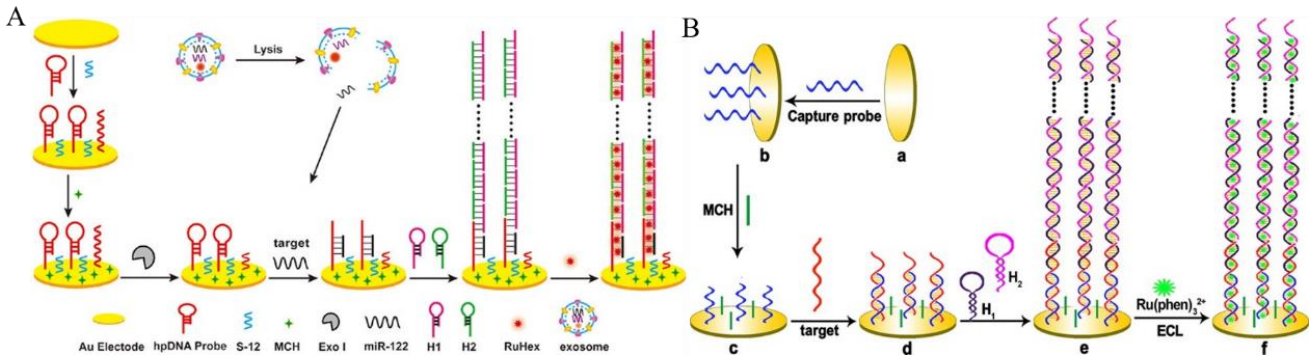

Figure 2. (**A**) Schematic illustration of the HCR electroanalytical assay for miRNA detection with reduced false-positive signals [49]. Copyright 2020 American Chemical Society. (**B**) Illustration of the universal and highly sensitive HCR-based Strategy for ECL detection of DNA [50]. Copyright 2012 American Chemical Society.

To further enhance the sensitivity, nanomaterials with high surface area are utilized for signal amplification. Trigger DNA enriched on nanomaterials can induce HCR with more accessibility and binding sites, and one target recognition event can be converted multi-HCR amplification reaction [52, 53]. For example, Zhu et al. reported a multiple amplified electrochemical method for microRNA-21 detection by using hierarchical flower-like gold nanostructures and spherical nucleic acids gold nanoparticles (SNAs AuNPs) [54]. Song et al. employed multiwalled carbon nanotubes as the DNA initiator strand carriers for cancer marker EBNA-1 detection [55]. Wang et al. developed an electrochemical biosensor for the determination of telomerase activity by using SNAs AuNPs-assisted mimic-HCR for dual signal amplification [56]. As demonstrated in Figure 3A, after the extension by telomerase, SNAs AuNPs were captured by the telomeric repeats on the electrode surface. Then, numerous DNA strands on AuNPs stimulated the mimic-HCR. A large number of positive charged RuHeX ions were intercalated into the DNA helixe to produce an amplified electrochemical signal.

Due to their high surface area and large load capacity, porous nanomaterials such as mesoporous silica nanoparticles (MSNs) and metal organic frameworks (MOFs) are usually applied in the fields of drug delivery and biosensing. Cheng et al. constructed a low background electrochemical sensing platform for mRNA detection by target-responsive HCR and controlled-release of electroactive cargo [57]. As shown in Figure 3B, electroactive MetB molecules were enclosed into MSNs and blocked by dsDNA. In the presence of minute target mRNA, multiple 5'-PO_4 cDNA were hydrolyzed under λ-Exo-aided target cycling. The released trigger DNA could induce the HCR reaction and numerous released MetB molecules that were intercalated into the minor groove of the formed DNA polymers, thus generating an enhanced signal with low background current. Similarly, they employed catalytic hairpin

assembly (CHA) to amplify the amount of trigger DNA for microRNA detection [58]. In addition, Han et al. used DNA microcapsules to carry MetB molecules for polychlorinated biphenyls detection [59]. After the binding of target and its aptamer, the released DNA would induce the nonlinear HCR reaction to form branched DNA dendrimers and the released MetB molecules were adsorbed to produce enhanced electrochemical responses. Although the redox probe has stable chemical properties, the current of the sensor is relatively small and the sensitivity is low, which limit the improvement of the sensor performance.

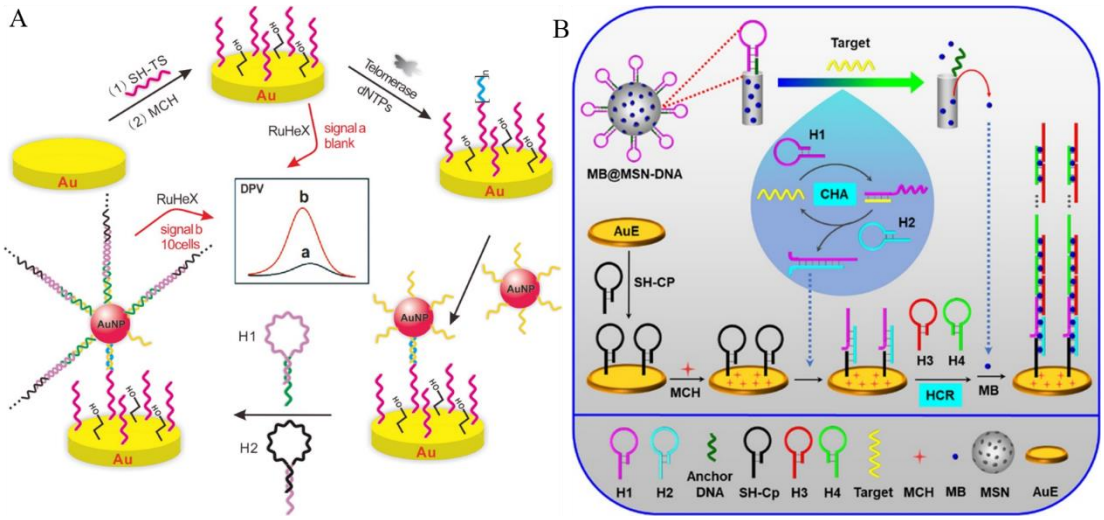

Figure 3. (**A**) Schematic illustration of SNAs AuNPs triggered mimic-HCR dual signal amplification electrochemical assay for telomerase activity detection [56]. Copyright 2015 American Chemical Society. (**B**) Illustration of mesoporous silica containers and programmed catalytic hairpin assembly/hybridization chain reaction based electrochemical sensing platform for miRNA ultrasensitive detection with low background [58]. Copyright 2019 American Chemical Society.

2.2 Redox molecules

To further enhance sensitivity, the enzyme-assisted amplification is usually integrated with HCR-based electrochemical methods. Moreover, the highly ordered DNA helix makes a large number of enzymes being arranged with precisely controlled density for higher amplification efficiency. For example, redox-reactive horseradish peroxidase (HRP) can catalyze the reduction of H_2O_2 in the presence or absence of redox probes alongside with the production of typical electrochemical signals [60]. Bai et al. reported an amperometric aptasensor for the detection of thrombin using HRP-mediated direct electrochemistry [61]. In this study, the capture probe was immobilized on the AuNPs-modified electrode and then hybridized with the complementary thrombin aptamer. Under the exonuclease-assisted target recycling, minute thrombin could induce the digestion of many aptamers and leave free capture probe to initiate HCR reaction. Then, numerous avidin-labeled HRPs were bound to the formed biotin-labeled dsDNA wires and produced an electrochemical signal through the direct electrochemistry that could be further amplified by the inherent electrocatalysis of HRP through H_2O_2. Besides, mediators (such as hydroquinol and o-phenylenediamine) can be introduced into the enzyme catalytic reaction to

shuttle electron transfer between electroactive center of HRP and to electrode surface, thus providing an enhanced electrochemical signal [62, 63]. Ge et al. developed a tetrahedral DNA nanostructure-based electrochemical biosensor for the detection of microRNA by HCR amplification [64]. As shown in Figure 4, DNA tetrahedron nanostructure (DTN) was used as a scaffold to immobilize bioprobes with well-adjusted distance and better orientation. After the hybridization and HCR reaction, multiple HRP enzymes were captured by DNA concatamer and generated the amplified electrochemical signal through the catalytic reaction between TMB and H_2O_2. Based on the highly ordered enzyme in the HCR product, the detection limit was improved to 100 aM for DNA detection. However, long dsDNA polymers from traditional HCR with linear self-assembly have a limited charge transfer capability because of the long distance between electrochemical species and the electrode. Therefore, different shaped DNA units have been introduced into HCR reaction. For example, Wang et al. reported an electrochemical aptasensor for tumorous exosomes detection based on the multidirectional HCR amplification [65]. In this work, H shape-like DNA units were employed to assemble the large DNA dendrimers. Numerous captured HRP molecules catalyzed the oxidation of TMB and produced a strong reduction current. Moreover, Jia et al. fabricated a DNA dendrimer with branched chain from nonlinear HCR and applied it to detect DNA by using HRP to catalyze redox reaction [30]. Graphene oxide-AuNPs nanocomposite was also used by Shuai et al. as a signal amplification carrier for HCR and HRP [66].

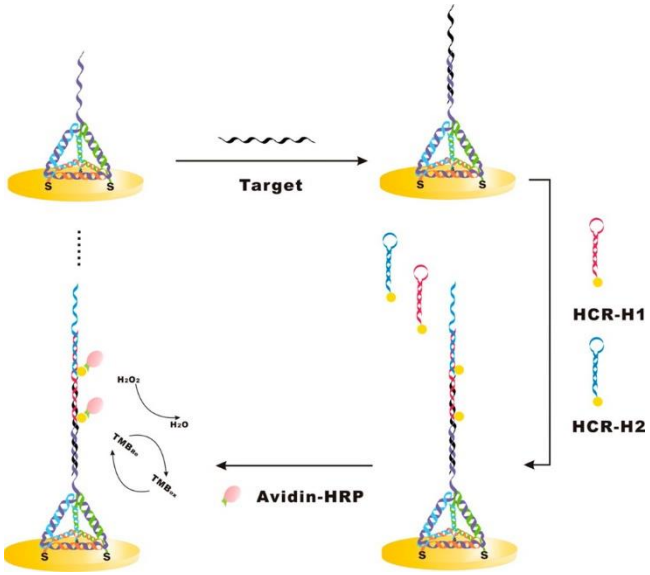

Figure 4. Schematic illustration of HCR amplification of microRNA detection with a tetrahedral DNA nanostructure-based electrochemical biosensor [64]. Copyright 2014 American Chemical Society.

Alkaline phosphatase (ALP) can convert electro-inactive 1-naphthyl phosphate into an electroactive derivative 1-naphthol that can produce an obvious electrochemical signal by DPV. Thus, streptavidin-alkaline phosphatase (SA-ALP) is used in HCR-based electrochemical methods [67, 68]. For example, Zhao et al. fabricated an electrochemical aptasensor for interferon-gamma detection based on HCR and ALP-signal amplification [69]. Wang et al. designed a novel strategy by integrating HCR with circular strand-displacement polymerase reaction (CSDPR) and ALP catalysis for the detection of

DNA [70]. However, extra enzyme modification, instability and harsh reaction conditions significantly limit the applications of enzyme-based electrochemical biosensors.

2.3 Mimic enzymes

Actually, only small portion of the enzyme (around 2–4 amino acids) is directly involved in enzyme catalysis. Thus, scientists have put great efforts to design and screen several molecules with enzyme-like properties as enzyme mimics. Among them, metal complexes have received a lot of attention, due to their enzyme-mimic catalytic capability and the intercalation into DNA structures [71]. For instance, copper (II) complexes can catalyze the reaction between TMB and H_2O_2; the principle was utilized for microRNA detection in combination with HCR and nanozyme [72]. Kou et al. employed manganese porphyrin (MnPP)-intercalating DNA nanoladders as the enhancers for the detection of matrix metalloproteinase-7 (MMP-7) [73]. As displayed in Figure 5, platinum nanoparticles (PtNPs) labeled with a peptide substrate and DNA S1 (P1-PtNPs-S1) were used as the recognition nanoprobes immobilized on the electrode. S1 on PtNPs hybridized with DNA1 (I1) and DNA2 (I2), and then triggered two HCRs to form DNA nanoladders. MnPP as peroxidase mimic was intercalated into the grooves of dsDNA nanowires and catalyzed the generation of insoluble precipitation on the electrode, thus leading to a weak DPV signal. However, in the presence of MMP-7, the peptide was cleaved and the PtNPs-S1 bioconjugate was liberated from the electrode, causing the decrease of numerous DNA nanoladders and the recovery of DPV signals.

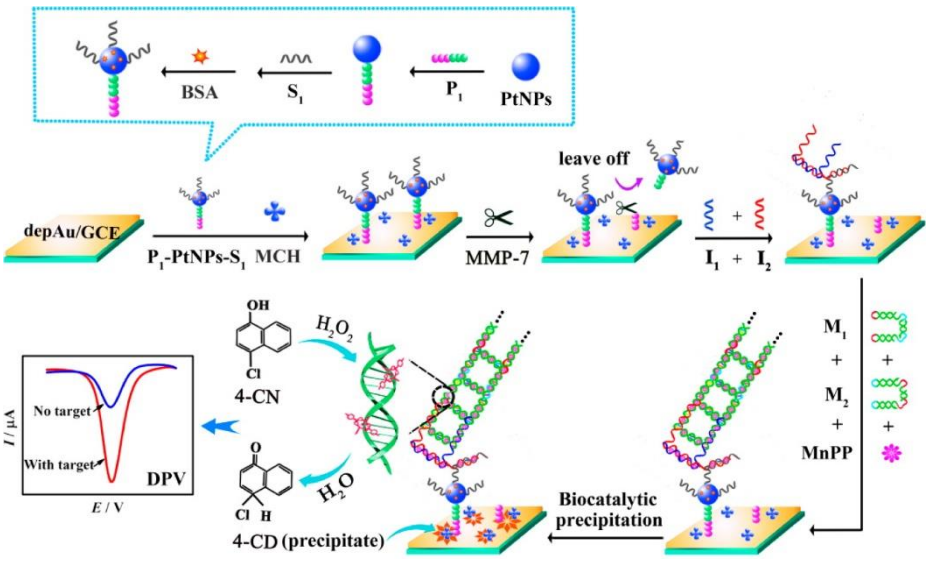

Figure 5. Schematic Illustrations of electrochemical biosensor for matrix metalloproteinase-7 detection with DNA enzyme decorated DNA nanoladders as enhancer [73]. Copyright 2016 American Chemical Society.

Hemin-based G-quadruplex complexes with peroxidase-like activity have been extensively applied in the construction of biosensors. The DNAzyme is more simple and stable than protein enzymes.

Moreover, the hemin-binding aptamer can be integrated into the herapin sequence without the interference of hybridization. After HCR, in situ self-assembled hemin/G-quadruplex complexes are cascaded through the formation of long nanowires as the electrocatalysts, efficiently achieving the secondary signal amplification process [74-76]. For this view, Yu et al. reported an electrochemical method for the detection of avian influenza A (H7N9) virus DNA by using hemin/G-quadruplexs in DNA concatamer to catalyze the oxidization of TMB by H_2O_2 [77]. Hou et al. found that hemin/G-quadruplex could catalyze the oxidation of 4-choloro-1-naphthol (4-CN) into insoluble product (benzo-4-chlorohexadienone) on the surface of the electrode, resulting in the suppression of the electron transfer between the electroactive species and the electrode [78]. Based on this detection principle, they reported an impedimetric immunoassay by using hemin/G-quadruplex DNAzyme nanowires on AuNPs [79]. In the presence of H_2O_2, hemin/G-quadruplex can catalyze the polymerization of aniline monomer into polyaniline (PAn) under very mild conditions [80]. The formed PAn can electrostatically adsorb along with dsDNA and generate high catalytic currents. For example, Zhang et al. reported an amplified electrochemical sensing of Pb^{2+} based on hemin/G-quadruplex-catalyzed deposition of PAn [81]. However, it is fussy to add redox mediator for signal output. In addition, nanomaterials have been employed to carry hemin/G-quadruplex-containing DNA concatamers for increasing the sensitivity of biosensors [82]. For instance, Fe-MOFs were used to load numerous hemin/G-quadruplexes from HCR and HRP to label human liver hepatocellular carcinoma cells by catalyzing the oxidation of hydroquinone (HQ) in the presence of H_2O_2 for signal amplification [83].

Besides as a catalyst, electroactive hemin can be explored as a signal donor based on the reversible redox of Fe(III)/Fe(II). Thus, numerous hemin/G-quadruplex complexes in HCR products can directly produce an amplified electrochemical signal by DPV [84-88]. Peng et al. developed a simple and sensitive method for the determination of rare circulating tumor cells (CTCs) [89]. As shown in Figure 6A, two complementary hairpins (HP1 and HP2) enclosed the G-quadruplex sequences at their ends that are divided into two pieces to restrain the nonspecific formation of the G-quadruplexes. The aptamer against EpCAM was inserted into the identification probe (IP). In the presence of EpCAM-expressing CTCs, the strong affinity binding of the aptamer and EpCAM on the surface of CTCs made the hairpin structure unfolding to hybridize with HP0. The formed IP/HP0 complex with three functional tails initiated the HCR reaction and bound to the hairpin-bearing tetrahedral DNA nanostructure (TDN) on the disposable screen-printed gold electrode (SPGE). After the addition of hemin, split G-quadruplex sequences in close proximity were transformed into lots of G-quadruplex/hemin complexes, producing a pronounced electrochemical signal. Furthermore, through the strand displacement reaction, those grasped CTCs could be released with a little damage for next clinical experiments. According to previous reports, G-quadruplexes can self-assemble into stable and well-defined G-quadruplex wire superstructure which retains the ability to bind with hemin [90, 91]. To pursue the higher sensitivity, Xu et al. presented an ingenious principle by integrating HCR with terminal deoxynucleotidyl transferase (TdT)-promoted polymerization and G-quadruplex wire for miRNA-21 detection (Figure 6B) [92]. In this work, HCR was conducted in homogeneous solution to precisely control conditions and achieve high reaction kinetics. Target miRNA-21 was hybridized with capture probe (CP) on the electrode. The exposed tail could capture the formed DNA concatamers with many biotin moieties as the main body structure that was further grafted with long G-quadruplex tail to form TdT-catalyzed polymerization into

branch structures through the SA-biotin interaction. Then, abundant G-quadruplexes were assembled into well-defined G-quadruplex wire superstructures. Finally, this method achieved a low detection limit of 0.2 fM and a wide detection range from 10 fM to 100 nM.

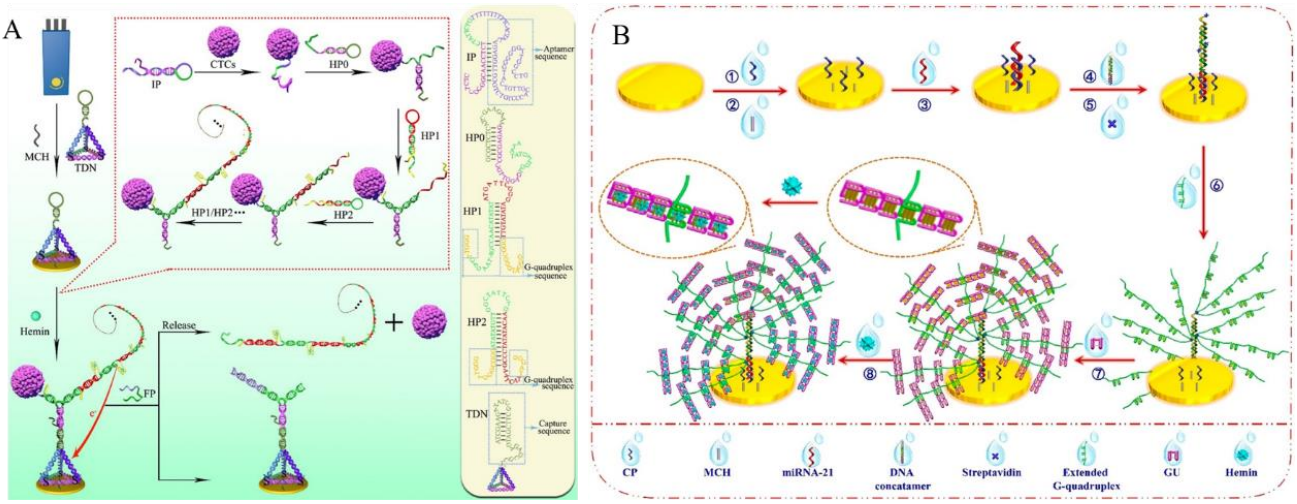

Figure 6. (**A**) Schematic interpretation of the controlled capture and release of CTCs on the electrode surface [89]. Copyright 2020 American Chemical Society. (**B**) Schematic diagram of the electrochemical DNA biosensor based on multibranched DNA nanoarchitectures for amplified electrochemical determination of miRNA-21 [92]. Copyright 2019 American Chemical Society.

2.4 Nanomaterials

Recently, nanomaterials have been widely used in electrochemical biosensors due to these intriguing properties, for instance, facile surface functionalization, high catalytic ability and well biocompatibility. Because of their large surface area and excellent conductivity, nanomaterials, such as carbon-based and metal-based nanostructures, are used as electrode modifiers for facilitating biomolecules immobilization and increasing electron transfer [93]. For example, the nanocomposites of gold nanoparticle/polypyrrole-reduced graphene oxide were utilized to modify the electrode for microRNA-16 detection [94]. In this section, we mainly review the works that coupled HCR protocol with nanomaterials as signal reporters or enhancers for biosensing.

AgNPs can directly generate a well-defined sharp electrochemical peak at low-redox potentials without acid dissolution. NPs have been labeled at the ends of hairpins H1 and H2 and multiple NPs are captured during the HCR reaction [95]. For example, Miao et al. employed AgNPs-laoding hairpins to form DNA ploymers on the AuNPs for microRNA detection [96]. Ge et al. developed an ECL method for tumor cells and H_2O_2 detection by using hairpin DNA-labeled luminol/Au NPs for HCR [97]. Long DNA polymers from HCR can provide more binding site for capturing functional NPs after HCR. For example, two types of redox molecules-carried DNA-labeled Fe_3O_4 NPs were utilized to label DNA polymers through hybridization for simultaneously detection of microRNA-141 and microRNA-21 [98]. Sun et al. developed a microfluidic paper-based electrochemical biosensor for the analysis of glycoprotein ovalbumin (OVA) based on molecularly imprinted polymers (MIPs) and cerium dioxide (CeO_2) as a catalytic label [99]. As shown in Figure 7, MIPs containing 4-mercaptophenylboronic acid

could capture OVA, and boronic acid and DNA-functionalized SiO_2@AuNPs were further used to label the captured OVA. Then, multiple capture DNA probes on NPs initiated HCR. CeO_2 was attached on the formed DNA concatamer through an amidation reaction and acted as the redox-active catalytic amplifier to catalyze the conversion of 1-naphthol to naphthoquinone.

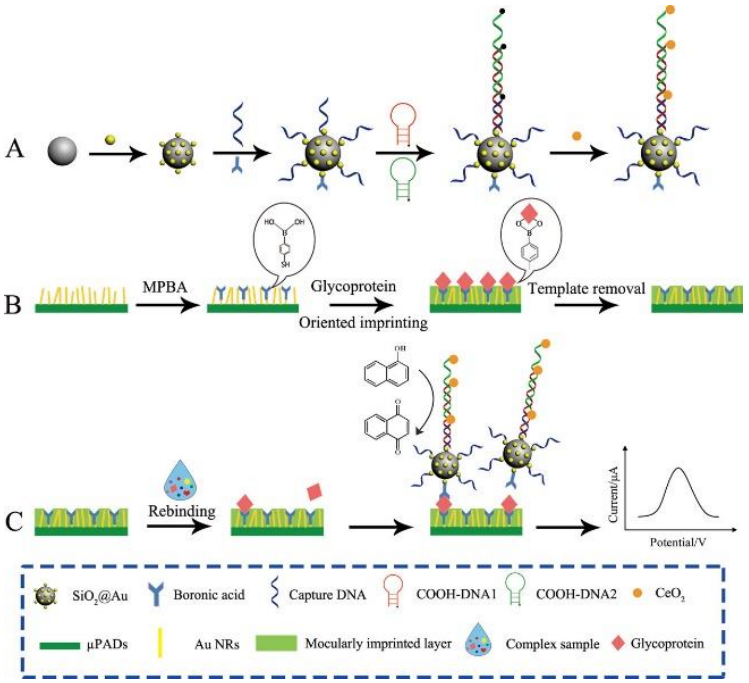

Figure 7. Schematic illustration of molecularly imprinted film and boronate affinity sandwich assay for glycoprotein detection [99]. Copyright 2019 American Chemical Society.

The HCR products (dsDNA superstructures) usually have high length, structural flexibility and negative charges. Thus, positively charged NPs can assemble along with dsDNA nanowires from HCR through the electrostatic interactions. It has been reported that the electrochemical signal from numerous Fc molecules in double-helix can be dramatically improved by the adsorbed AuNPs [100]. Moreover, positively charged Ag@Au core-shell NPs exhibited higher enhancement efficiency than solo AgNP and AuNP because of the localized electric field enhancement [101]. Chen et al. reported an electrochemical prostate-specific antigen (PSA) detection by using DNA concatemer-AgNPs as the signal probes [102]. In this study, in the presence of PSA, HCR occurred on the sandwich immune-structure. Numerous AgNPs with positive charges were electrostatically adsorbed on the dsDNA polymers and produced a strong electrochemical signal. However, the method based on the electrostatic interaction always faces a common problem of low reproducibility.

It is attractive to utilize long HCR product dsDNA superstructure as a template for in situ formation of metal nanomaterials as signal tags for label-free detection [103]. For instance, Xie et al. proposed an ultrasensitive electrochemical biosensor for Pb^{2+} detection based on dual triggers-induced decomposition of HCR DNA polymer-carried AgNPs [104]. In this paper, the branched DNA polymer from HCR on the electrode surface could carry a large number of AgNPs to produce a high current signal. However, with the aid of DNAzyme assisted target recycling and magnetic separation, Pb^{2+} could generate lots of substrate fragments. The released dual triggers could heavily decompose the branched

DNA polymer and caused an obvious current signal. Meanwhile, ssDNA with a specific sequence and structure can also be used as a template to synthesize silver nanocluster (AgNC) that contains several to tens Ag atoms and shows similar redox property like AgNP [105, 106]. Yang developed an ultrasensitive and label-free electrochemical biosensor for microRNA (miRNA-199a) detection based on cascade DNA signal amplification strategy and DNA-templated in situ generation of AgNCs [107]. As shown in Figure 8, through the target-assisted polymerization nicking reaction (TAPNR) amplification, minute miRNA-199a could produce lots of intermediate DNA that further initiated the HCR amplification on the sensing electrode. Then, the formed DNA concatemer with massive C-rich loop DNA templates could be used to synthesize AgNCs as electrochemical tags for next direct measurements. Based on the dual amplification strategy and in situ synthesized AgNCs, the detection limit of this method was down to 0.64 fM. In addition to the redox property, AgNCs also displays interesting ECL property. Zou et al. reported an ECL biosensor for the detection of histone acetyltransferases (HATs) activity by coupling HCR with AgNCs [108].

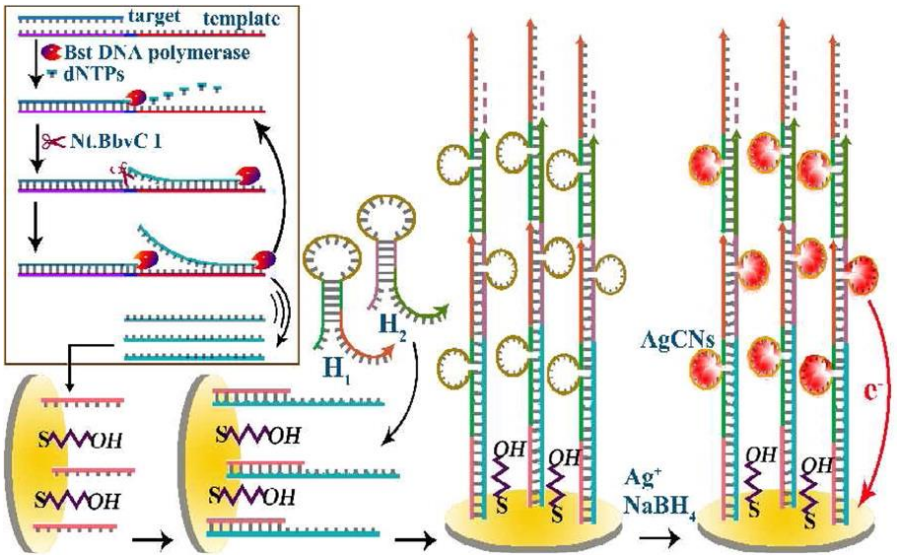

Figure 8. Schematic illustration of ultrasensitive and label-free electrochemical detection of miRNA-199a based on in situ generated AgNCs by coupling TAPNR with HCR amplifications [107]. Copyright 2015 American Chemical Society.

Unlike AgNCs, copper nanoparticles (CuNPs) can be selectively formed by using dsDNA as the template without the dependence on the specificity of DNA sequence [109]. Zhao et al. proposed an electrochemical method for folate receptor (FR) detection based on HCR-assisted formation of CuNPs [110]. In this work, the presence of FR could protect folate-functionalized DNA probe from the degradation by exonuclease I (Exo I) and the DNA probe further triggered HCR on the electrode surface. Long dsDNA oligomers from HCR acted as the templates for the in situ formation of CuNPs that could release large amounts of copper ions through acid dissolution, thus catalyzing the oxidation of o-phenylenediamine (OPD) by dissolved O_2 to produce strong electrochemical responses.

3. MAGNETIC NANOPARTICLES OR BEADS

Magnetic microbeads (MBs) or nanoparticles (MNPs) have been widely utilized in electrochemical bioassays, because they can separate the target from sample matrices through magnetic separation, indirectly increasing the concentration of target and reducing the background signal. Moreover, after the formation of sandwich complexes, MBs were accumulated and enriched on the electrode surface for next detection in the presence of the external magnet. This magnetic-controlled electrochemical methods avoid the delicate electrode preparation to confirm the well density and orientation of probes [111].

Generally, MBs serve as the scaffolds and separators for target conversion [112-114]. For this view, Zhang et al. proposed an immuno-HCR assay strategy for protein detection [115]. As presented in Figure 9A, MBs were modified with monoclonal mouse anti-human IgG (Ab_1), and AuNPs were functionalized with DNA initiator strands and polyclonal goat anti-human IgG (Ab_2). In the presence of target IgG, the sandwiched immunocomplexes were formed between Ab_1-MBs and Ab_2-AuNPs and plenty of initiators on AuNPs propagated the HCR reaction between Fc-labeled H1 and H2. After magnetic-controlled accumulation on the electrode, numerous Fc molecules produced an obvious electrochemical signal. Moreover, a protein converting strategy was proposed by Yang and co-workers for the detection of cystatin C [116]. As shown in Figure 9B, Au@Fe_3O_4 NPs were modified with DNA1-labeled Ab_1 (DNA1-Ab_1) and S1/DNA3 duplex, respectively. In the absence of cystatin C, DNA2 hardly hybridized with DNA3 because of the short complementary sequence. However, in the presence of cystatin C, the binding of target and antibody induced PLA-based strand displacement reaction to release S1. To further improve the conversion ratio, T7 Exo-aided SDA strategy was introduced. After the magnetic separation, S1 was sensitively detected by the HCR-based electrochemical method.

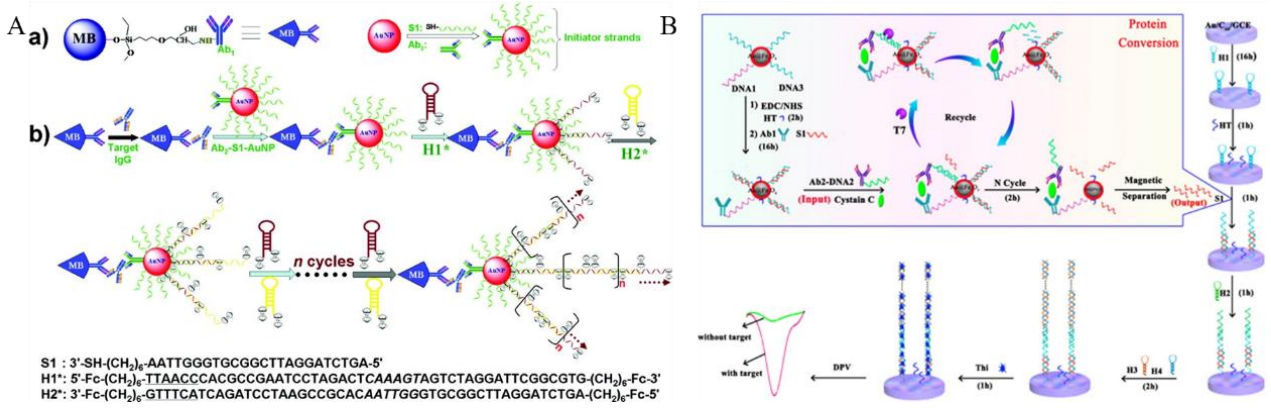

Figure 9. (**A**) Schematic interpretation of immuno-HCR assay method. a) Design and preparation of Ab_1-MBs and Ab_2-S1-AuNPs. b) Schematic depiction of the sandwiched immunoassays with the DNA-based HCR [115]. Copyright 2012 American Chemical Society. (**B**) Schematic interpretation of electrochemical detection of cystatin C by combining a protein converting strategy with T7 Exo-assisted protein cyclic enzymatic amplification [116]. Copyright 2016 American Chemical Society.

Besides magnetic separation, MB can also serve as the platform for immobilizing detection probe DNA and triggering homogeneous HCR signal amplification [117-121]. For instance, Torrente-Rodríguez et al. proposed a hybridization reaction in which HCR and HRP-catalyzed redox reactions happen on the surface of MBs for miRNA detection [122]. Yuan reported a proximity protein converting strategy for the detection of total protein of *Nosema bombycis* [123]. In this study, after the proximity immunoreaction, HCR reaction occurred on Au@Fe_3O_4 NPs and substantial MetB molecules were adsorbed on DNA polymers. After the separation and hydrolysis, the released MetB was determined by cucurbit(7)-uril /Au@Fe_3O_4NPs/GCE.

4. HOMOGENEOUS DETECTION

Most of electrochemical biosensors require the immobilization of biological recognition elements on the solid surface. They may exhibit the shortcomings of complicated immobilization process and time-consuming [124, 125]. Moreover, the activity and recognition ability of biomolecules and the efficiency of HCR were heavily suppressed because of local steric hindrance and bad orientation [126]. Therefore, it is grateful to develop simple and low-cost immobilization-free HCR-based electrochemical biosensors for bioassays [127, 128]. Typically, Li et al. designed a label-free HCR-based homogenous electrochemical method for miRNA detection [129]. As illustrated in Figure 10, miRNA induced the continuous HCR of two types of metastable DNA units with split G-quadruplex sequences and multiple G-quadruplexes were formed alongside with DNA concatamers. Lots of MetB molecules are intercalated into the dsDNA chains and G-quadruplexes, subsequently blocking the access to the electrode surface and greatly decreasing the diffusion current. Furthermore, Liao et al. reported a label-free and immobilization-free homogeneous electrochemical aptasensor for thrombin detection by combing proxHCR with in situ formation of G-quadruplexes [130].

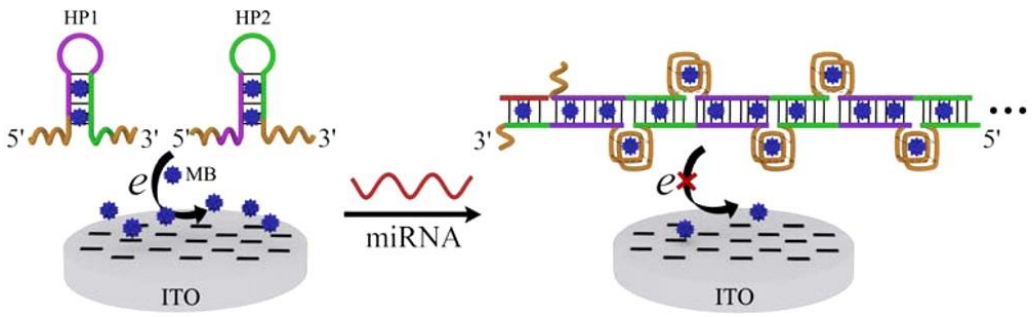

Figure 10. Schematic illustration of the label-free and enzyme-free homogeneous electrochemical strategy based on HCR amplification for miRNA assay [129]. Copyright 2015 American Chemical Society.

5. RATIOMETRIC METHOD

Most of the reported single-singaling output electrochemical methods may suffer from false negative or positive results because of inevitable disturbance from environmental and experimental conditions. Therefore, it is desirable to develop ratiometric methods that can endow the assays with enhanced sensitivity and accuracy by eliminating intrinsic errors [131, 132]. Metallization on ssDNA template can destroy the ssDNA recognition and hybridization capabilities. Liu et al. demonstrated that glutathione (GSH) could liberate ssDNA from metallization via the interaction between thiol groups and AgNPs and facilitate the occurrence of HCR amplification for ratiometric biosensing GSH [133]. In this work, the deposited AgNPs were liberated from the DNA initiators in the presence of GSH, and the in situ HCR was triggered to form a long DNA polymer. Then, MetB molecules were intercalated into the duplex. With the increasing concentration of GSH, the peak current from MetB (I_{MetB}) was increased and that of AgNPs (I_{MetB}) was reduced. Finally, by recording the ratiometric signal (I_{MetB}/I_{Ag}), the intracellular level of GSH was sensitively monitored, indirectly evaluating intracellular redox homeostasis. Meanwhile, ratiometric methods based on redox-labeled capture probe DNA and molecules-intercalated HCR product were also developed [134, 135]. For example, Yuan et al. reported a ratiometric electrochemical method for microRNA detection based on duplex-specific nuclease (DSN) and HCR for dual signal amplification [136]. In this study, Fc-labeled hairpin capture DNA was immobilized on the electrode. When the target microRNA was added to hybridize with the capture DNA probe, DSN-catalyzed target recycling reaction was triggered and numerous Fc molecules were released from the electrode, resulting in the decrease of electrochemical signal. Then, the residual pieces initiated the HCR to form DNA polymers to bind DNA and thionine-conjugated AuNPs through hybridization, thus resulting in the signal-enhancement of thionine.

Tumor exosomes are promising biomarkers for early cancer diagnosis in a noninvasive manner and their surface has various proteins that can be used as the targets for bio-recognition. Yang et al. developed an immobilization-free hyperbranched HCR-based ratiometric electrochemical strategy for tumor exosome capture and determination [137]. As illustrated in Figure 11, Fe_3O_4@SiO_2 NPs were functionalized with MUC1 aptamer and CD63 aptamer, respectively. After the capture and separation, exosomes were labeled with cholesterol-modified DNA initiators via the hydrophobic interaction between cholesterol and the phospholipin bilay. After the second magnetic isolation, two hairpins-labeled DTNs were added to the NPs-exosomes-DNA initiator to trigger hyperbranched HCR. Numerous $Ru(NH_3)_6^{3+}$ (Ru(III)) ions were adsorbed on the generated sandwich complexes and only a small amount of them remained in solution after the magnetic separation. The inhibition of the redox reaction between Ru(III) and $[Fe(CN)_6]^{3-}$ (Fe(III)) resulted in the change of $I_{Fe(III)}/I_{Ru(III)}$ value.

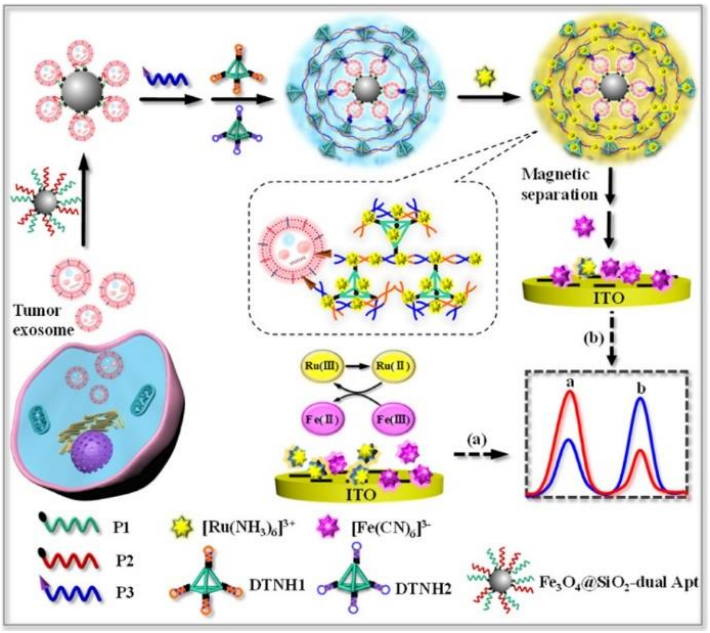

Figure 11. Schematic illustration of the ratiometric immobilization-free electrochemical sensing system for tumor exosome detection (a) in the absence and (b) in the presence of the tumor exosomes [137]. Copyright 2021 American Chemical Society.

6. CONCLUSION

Thanks to the merits of high sensitivity, enzyme-free and isothermal amplification, many novel and powerful HCR-based methods have been successfully developed for bioassays. In this review, we summarized the HCR-based amplification strategies for electrochemical biosensors according to the type of signal reporters. Although nanomaterials plus HCR have been widely used for the signal amplification, the limited stability and complicated preparation procedure seriously suppress their practical applications. To further improve the sensitivity, several enzyme-aided amplification strategies are well coupled to HCR. However, the vulnerability of enzymes may limit the applications of these biosensors in complicated real lives. Therefore, the development of enzyme-free HCR-based electrochemical biosensors is still attractive, such as non-linear HCR and other enzyme-free DNA signal amplification strategies.

ACKOWLEDGMENTS
This work was supported by the Hunan Provincial Natural Science Foundation of China (NO. 2019JJ70038).

References

1. S. Khan, B. Burciu, C. D. M. Filipe, Y. Li, K. Dellinger and T. F. Didar, *ACS Nano*, 15 (2021) 13943.
2. M. Li, F. Yin, L. Song, X. Mao, F. Li, C. Fan, X. Zuo and Q. Xia, *Chem. Rev.*, 121 (2021)

10469.
3. C. Chen, Y. Feng, X. Xia, M. La and B. Zhou, *Int. J. Electrochem. Sci.*, 14 (2019) 5174.
4. R. M. Dirks and N. A. Pierce, *Proc. Natl. Acad. Sci. USA*, 101 (2004) 15275.
5. D. Yang, Y. Tang and P. Miao, *TrAC-Trend. Anal. Chem.*, 94 (2017) 1.
6. E. E. Augspurger, M. Rana and M. V. Yigit, *ACS Sens.*, 3 (2018) 878.
7. C. Zhang, J. Chen, R. Sun, Z. Huang, Z. Luo, C. Zhou, M. Wu, Y. Duan and Y. Li, *ACS Sens.*, 5 (2020) 2977.
8. H. Chai, W. Cheng, D. Jin and P. Miao, *ACS Appl Mater Interfaces*, 13 (2021) 38931.
9. T. Sun, Y. Guo and F. Zhao, *Int. J. Electrochem. Sci.*, 16 (2021) 210732.
10. Y. Yang, X. Liu, M. Wu, X. Wang, T. Hou and F. Li, *Sens. Actuat. B: Chem.*, 236 (2016) 597.
11. F. Zhai, Q. Yu, H. Zhou, J. Liu, W. Yang and J. You, *J. Electroanal. Chem.*, 837 (2019) 137.
12. L. P. Jia, L. J. Wang, R. N. Ma, L. Shang, W. Zhang, Q. W. Xue and H. S. Wang, *Talanta*, 179 (2018) 414.
13. L. P. Jia, R. N. Zhao, L. J. Wang, R. N. Ma, W. Zhang, L. Shang and H. S. Wang, *Biosens. Bioelectron.*, 117 (2018) 690.
14. C. Gan, B. Wang, J. Huang, A. Qileng, Z. He, H. Lei, W. Liu and Y. Liu, *Biosens. Bioelectron.*, 98 (2017) 126.
15. X. Li, J. Li, C. Zhu, X. Zhang and J. Chen, *Talanta*, 182 (2018) 292.
16. Q. Wang, Y. Song, Y. Chai, G. Pan, T. Li, Y. Yuan and R. Yuan, *Biosens. Bioelectron.*, 60 (2014) 118.
17. X. Gu, K. Wang, J. Qiu, Y. Wang, S. Tian, Z. He, R. Zong and H.-B. Kraatz, *Sens. Actuat. B: Chem.*, 334 (2021) 129674.
18. L. Tong, J. Wu, J. Li, H. Ju and F. Yan, *Analyst*, 138 (2013) 4870.
19. J. Hu, Y. Yu, J. C. Brooks, L. A. Godwin, S. Somasundaram, F. Torabinejad, J. Kim, C. Shannon and C. J. Easley, *J. Am. Chem. Soc.*, 136 (2014) 8467.
20. B. Koos, G. Cane, K. Grannas, L. Lof, L. Arngarden, J. Heldin, C. M. Clausson, A. Klaesson, M. K. Hirvonen, F. M. de Oliveira, V. O. Talibov, N. T. Pham, M. Auer, U. H. Danielson, J. Haybaeck, M. Kamali-Moghaddam and O. Soderberg, *Nat. Commun.*, 6 (2015) 7294.
21. S. Liu, Y. Wang, J. Ming, Y. Lin, C. Cheng and F. Li, *Biosens. Bioelectron.*, 49 (2013) 472.
22. X. Wu, Y. Chai, R. Yuan, Y. Zhuo and Y. Chen, *Sens. Actuat. B: Chem.*, 203 (2014) 296.
23. T. Bao, W. Wen, X. Zhang, Q. Xia and S. Wang, *Biosens. Bioelectron.*, 70 (2015) 318.
24. F. Hong, X. Chen, Y. Cao, Y. Dong, D. Wu, F. Hu and N. Gan, *Biosens. Bioelectron.*, 112 (2018) 202.
25. Y. Wang, J. Zheng, C. Duan, J. Jiao, Y. Gong, H. Shi and Y. Xiang, *Analyst*, 146 (2021) 1355.
26. Z. Zhu, J. Lei, L. Liu and H. Ju, *Analyst*, 138 (2013) 5995.
27. Y. Huang, M. Tao, S. Luo, Y. Zhang, B. Situ, X. Ye, P. Chen, X. Jiang, Q. Wang and L. Zheng, *Anal. Chim. Acta*, 1107 (2020) 40.
28. W. Li, D. Zhao, D. Tian, M. Zhai, H. Xu, L. Zheng, S. Li and Y. Sang, *J. Electroanal. Chem.*, 895 (2021) 115447.
29. L. Zhou, Y. Wang, C. Yang, H. Xu, J. Luo, W. Zhang, X. Tang, S. Yang, W. Fu, K. Chang and M. Chen, *Biosens. Bioelectron.*, 126 (2019) 657.
30. L. Jia, S. Shi, R. Ma, W. Jia and H. Wang, *Biosens. Bioelectron.*, 80 (2016) 392.
31. S. Liu, Y. Lin, T. Liu, C. Cheng, W. Wei, L. Wang and F. Li, *Biosens. Bioelectron.*, 56 (2014) 12.
32. Y. Jiang, X. Chen, N. Feng and P. Miao, *Sens. Actuat. B: Chem.*, 340 (2021) 129952.
33. D. Yang, L. Ning, T. Gao, Z. Ye and G. Li, *Electrochem. Commun.*, 58 (2015) 33.
34. M. Hong, M. Wang, J. Wang, X. Xu and Z. Lin, *Biosens. Bioelectron.*, 94 (2017) 19.
35. Y. Wang, M. Li and Y. Zhang, *Analyst*, 146 (2021) 2886.
36. B. Han, L. Dong, L. Li, L. Sha, Y. Cao and J. Zhao, *Sens. Actuat. B: Chem.*, 325 (2020) 128762.

37. X. Li, G. Peng, F. Cui, Q. Qiu, X. Chen and H. Huang, *Biosens. Bioelectron.*, 113 (2018) 116.
38. Q. Zhu, Y. Chai, Y. Zhuo and R. Yuan, *Biosens. Bioelectron.*, 68 (2015) 42.
39. W. Ren, Z. F. Gao, N. B. Li and H. Q. Luo, *Biosens. Bioelectron.*, 63 (2015) 153.
40. J. Jiang, H. Wu, Y. Su, Y. Liang, B. Shu and C. Zhang, *Anal. Chem.*, 92 (2020) 7708.
41. Y. H. Cheng, S. J. Liu and J. H. Jiang, *Talanta*, 222 (2021) 121536.
42. S. Liu, L. Fang, Y. Wang and L. Wang, *Anal. Chem.*, 89 (2017) 3108.
43. Y. Wang, L. Jiang, Q. Leng, Y. Wu, X. He and K. Wang, *Biosens. Bioelectron.*, 77 (2016) 914.
44. Y. Yang, G. Yang, H. Chen, H. Zhang, J. J. Feng and C. Cai, *Analyst*, 143 (2018) 2051.
45. C. Gu, X. Kong, X. Liu, P. Gai and F. Li, *Anal. Chem.*, 91 (2019) 8697.
46. H. Yang, Y. Gao, S. Wang, Y. Qin, L. Xu, D. Jin, F. Yang and G. J. Zhang, *Biosens. Bioelectron.*, 80 (2016) 450.
47. R. Zeng, L. Su, Z. Luo, L. Zhang, M. Lu and D. Tang, *Anal. Chim. Acta*, 1038 (2018) 21.
48. J. Guo, J. Wang, J. Zhang, W. Zhang and Y. Zhang, *Biosens. Bioelectron.*, 90 (2017) 159.
49. Q. Guo, Y. Yu, H. Zhang, C. Cai and Q. Shen, *Anal. Chem.*, 92 (2020) 5302.
50. Y. Chen, J. Xu, J. Su, Y. Xiang, R. Yuan and Y. Chai, *Anal. Chem.*, 84 (2012) 7750.
51. X. Huang, Y. Zhang, W. Xu, W. Xu, L. Guo, B. Qiu and Z. Lin, *Chem. Commun.*, 55 (2019) 12980.
52. Y. Chang, Y. Chai, S. Xie, Y. Yuan, J. Zhang and R. Yuan, *Analyst*, 139 (2014) 4264.
53. J. Lu, L. Wu, Y. Hu, S. Wang and Z. Guo, *Biosens. Bioelectron.*, 109 (2018) 13.
54. D. Zhu, W. Liu, W. Cao, J. Chao, S. Su, L. Wang and C. Fan, *Electroanalysis*, 30 (2018) 1349.
55. C. Song, G. Xie, L. Wang, L. Liu, G. Tian and H. Xiang, *Biosens. Bioelectron.*, 58 (2014) 68.
56. W. J. Wang, J. J. Li, K. Rui, P. P. Gai, J. R. Zhang and J. J. Zhu, *Anal. Chem.*, 87 (2015) 3019.
57. H. Cheng, J. Liu, W. Ma, S. Duan, J. Huang, X. He and K. Wang, *Anal. Chem.*, 90 (2018) 12544.
58. H. Cheng, W. Li, S. Duan, J. Peng, J. Liu, W. Ma, H. Wang, X. He and K. Wang, *Anal. Chem.*, 91 (2019) 10672.
59. T. Han, S. Wang, F. Sheng, S. Wang, T. Dai, X. Zhang and G. Wang, *Analyst*, 145 (2020) 3598.
60. J. Fu, J. Wu, R. Zhang, Q. Wu and H. Ju, *Sens. Actuat. B: Chem.*, 345 (2021) 130436.
61. L. Bai, Y. Chai, R. Yuan, Y. Yuan, S. Xie and L. Jiang, *Biosens. Bioelectron.*, 50 (2013) 325.
62. X. Liu, H.-L. Shuai, Y.-J. Liu and K.-J. Huang, *Sens. Actuat. B: Chem.*, 235 (2016) 603.
63. Y. X. Chen, K. J. Huang, L. L. He and Y. H. Wang, *Biosens. Bioelectron.*, 100 (2018) 274.
64. Z. Ge, M. Lin, P. Wang, H. Pei, J. Yan, J. Shi, Q. Huang, D. He, C. Fan and X. Zuo, *Anal. Chem.*, 86 (2014) 2124.
65. L. Wang, L. Zeng, Y. Wang, T. Chen, W. Chen, G. Chen, C. Li and J. Chen, *Sens. Actuat. B: Chem.*, 332 (2021) 129471.
66. H. L. Shuai, X. Wu, K. J. Huang and Z. B. Zhai, *Biosens. Bioelectron.*, 94 (2017) 616.
67. Q. Zhai, Y. He, X. Li, J. Guo, S. Li and G. Yi, *J. Electroanal. Chem.*, 758 (2015) 20.
68. S. Luo, Y. Zhang, G. Huang, B. Situ, X. Ye, M. Tao, Y. Huang, B. Li, X. Jiang, Q. Wang and L. Zheng, *Sens. Actuat. B: Chem.*, 338 (2021) 129857.
69. J. Zhao, C. Chen, L. Zhang, J. Jiang and R. Yu, *Biosens. Bioelectron.*, 36 (2012) 129.
70. C. Wang, H. Zhou, W. Zhu, H. Li, J. Jiang, G. Shen and R. Yu, *Biosens. Bioelectron.*, 47 (2013) 324.
71. X. Zhou, S. Xue, P. Jing and W. Xu, *Biosens. Bioelectron.*, 86 (2016) 656.
72. L. Tian, J. Qi, O. Oderinde, C. Yao, W. Song and Y. Wang, *Biosens. Bioelectron.*, 110 (2018) 110.
73. B.-B. Kou, L. Zhang, H. Xie, D. Wang, Y.-L. Yuan, Y.-Q. Chai and R. Yuan, *ACS App. Mater. Interfaces*, 8 (2016) 22869.
74. K. Peng, H. Zhao, Y. Yuan, R. Yuan and X. Wu, *Biosens. Bioelectron.*, 55 (2014) 366.
75. J. Zhang, Y. Chai, R. Yuan, Y. Yuan, L. Bai, S. Xie and L. Jiang, *Analyst*, 138 (2013) 4558.
76. T. Bao, M. Wen, W. Wen, X. Zhang and S. Wang, *Sens. Actuat. B: Chem.*, 296 (2019) 126606.

77. Y. Yu, Z. Chen, W. Jian, D. Sun, B. Zhang, X. Li and M. Yao, *Biosens. Bioelectron.*, 64 (2015) 566.
78. L. Hou, Z. Gao, M. Xu, X. Cao, X. Wu, G. Chen and D. Tang, *Biosens. Bioelectron.*, 54 (2014) 365.
79. L. Hou, X. Wu, G. Chen, H. Yang, M. Lu and D. Tang, *Biosens. Bioelectron.*, 68 (2015) 487.
80. L. Ding, L. Zhang, H. Yang, H. Liu, S. Ge and J. Yu, *Sens. Actuat. B: Chem.*, 268 (2018) 210.
81. B. Zhang, J. Chen, B. Liu and D. Tang, *Biosens. Bioelectron.*, 69 (2015) 230.
82. L. Liu, C. Song, Z. Zhang, J. Yang, L. Zhou, X. Zhang and G. Xie, *Biosens. Bioelectron.*, 70 (2015) 351.
83. D. Chen, D. Sun, Z. Wang, W. Qin, L. Chen, L. Zhou and Y. Zhang, *Biosens. Bioelectron.*, 117 (2018) 416.
84. G. Xiang, D. Jiang, F. Luo, F. Liu, L. Liu and X. Pu, *Sens. Actuat. B: Chem.*, 195 (2014) 515.
85. C. Wang, Y. Qian, Y. Zhang, S. Meng, S. Wang, Y. Li and F. Gao, *Sens. Actuat. B: Chem.*, 238 (2017) 434.
86. X. Sun, H. Chen, S. Wang, Y. Zhang, Y. Tian and N. Zhou, *Anal. Chim. Acta*, 1021 (2018) 121.
87. Z. Liu, S. Lei, L. Zou, G. Li, L. Xu and B. Ye, *Biosens. Bioelectron.*, 131 (2019) 113.
88. B. Yao, S. Zhu, X. Xu, N. Feng, Y. Tian and N. Zhou, *Analyst*, 144 (2019) 2179.
89. Y. Peng, Y. Pan, Y. Han, Z. Sun, M. Jalalah, M. S. Al-Assiri, F. A. Harraz, J. Yang and G. Li, *Anal. Chem.*, 92 (2020) 13478.
90. N. M. Hessari, L. Spindler, T. Troha, W. C. Lam, I. Drevensek-Olenik and M. W. da Silva, *Chemistry*, 20 (2014) 3626.
91. Z. F. Gao, Y. L. Huang, W. Ren, H. Q. Luo and N. B. Li, *Biosens. Bioelectron.*, 78 (2016) 351.
92. J. Xu, C. Yan, X. Wang, B. Yao, J. Lu, G. Liu and W. Chen, *Anal. Chem.*, 91 (2019) 9747.
93. Y. Yu, C. Yu, R. Gao, J. Chen, H. Zhong, Y. Wen, X. Ji, J. Wu and J. He, *Biosens. Bioelectron.*, 131 (2019) 207.
94. J. Bao, C. Hou, Y. Zhao, X. Geng, M. Samalo, H. Yang, M. Bian and D. Huo, *Talanta*, 196 (2019) 329.
95. C. Mei, L. Pan, W. Xu, H. Xu, Y. Zhang, Z. Li, B. Dong, X. Ke, C. McAlinden, M. Yang, Q. Wang and J. Huang, *Sens. Actuat. B: Chem.*, 345 (2021) 130398.
96. P. Miao, Y. Tang and J. Yin, *Chem. Commun.*, 51 (2015) 15629.
97. S. Ge, J. Zhao, S. Wang, F. Lan, M. Yan and J. Yu, *Biosens. Bioelectron.*, 102 (2018) 411.
98. Y. H. Yuan, Y. D. Wu, B. Z. Chi, S. H. Wen, R. P. Liang and J. D. Qiu, *Biosens. Bioelectron.*, 97 (2017) 325.
99. X. Sun, Y. Jian, H. Wang, S. Ge, M. Yan and J. Yu, *ACS Appl. Mater. Interfaces*, 11 (2019) 16198.
100. Z. Li, X. Miao, K. Xing, A. Zhu and L. Ling, *Biosens. Bioelectron.*, 74 (2015) 687.
101. Z. Li, X. Miao, K. Xing, X. Peng, A. Zhu and L. Ling, *Biosens. Bioelectron.*, 80 (2016) 339.
102. X. Chen, Y. Wang, J. Zhang and Y. Zhang, *Analyst*, 144 (2019) 6313.
103. C. Feng, J. Guo, G. Li, B. Ye and L. Zou, *Sens. Actuat. B: Chem.*, 326 (2021) 129437.
104. X. Xie, Y. Chai, Y. Yuan and R. Yuan, *Anal. Chim. Acta*, 1034 (2018) 56.
105. Z. Chen, Y. Liu, C. Xin, J. Zhao and S. Liu, *Biosens. Bioelectron.*, 113 (2018) 1.
106. X. Peng, J. Zhu, W. Wen, T. Bao, X. Zhang, H. He and S. Wang, *Biosens. Bioelectron.*, 118 (2018) 174.
107. C. Yang, K. Shi, B. Dou, Y. Xiang, Y. Chai and R. Yuan, *ACS Appl. Mater. Interfaces*, 7 (2015) 1188.
108. Y. Zou, H. Zhang, Z. Wang, Q. Liu and Y. Liu, *Talanta*, 198 (2019) 39.
109. Y. Wang, X. Zhang, L. Zhao, T. Bao, W. Wen, X. Zhang and S. Wang, *Biosens. Bioelectron.*, 98 (2017) 386.
110. J. Zhao, S. Hu, Y. Cao, B. Zhang and G. Li, *Biosens. Bioelectron.*, 66 (2015) 327.
111. F. Qiu, X. Gan, B. Jiang, R. Yuan and Y. Xiang, *Sens. Actuat. B: Chem.*, 331 (2021) 129395.

112. L. P. Jia, Z. Feng, R. N. Zhao, R. N. Ma, W. Zhang, L. Shang, W. L. Jia and H. S. Wang, *Analyst*, 145 (2020) 3605.
113. S. Zhao, J. Xiao, H. Wang, L. Li, K. Wang, J. Lv and Z. Zhang, *Anal. Chim. Acta*, 1181 (2021) 338908.
114. Y. Li, H. Liu, H. Huang, J. Deng, L. Fang, J. Luo, S. Zhang, J. Huang, W. Liang and J. Zheng, *Biosens. Bioelectron.*, 147 (2020) 111752.
115. B. Zhang, B. Liu, D. Tang, R. Niessner, G. Chen and D. Knopp, *Anal. Chem.*, 84 (2012) 5392.
116. Z. H. Yang, Y. Zhuo, R. Yuan and Y. Q. Chai, *Anal. Chem.*, 88 (2016) 5189.
117. J. Zhuang, L. Fu, M. Xu, Q. Zhou, G. Chen and D. Tang, *Biosens. Bioelectron.*, 45 (2013) 52.
118. Y. Zhang, H. Li, M. Chen, X. Fang, P. Pang, H. Wang, Z. Wu and W. Yang, *Sens. Actuat. B: Chem.*, 249 (2017) 431.
119. W. J. Guo, Z. Wu, X. Y. Yang, D. W. Pang and Z. L. Zhang, *Biosens. Bioelectron.*, 131 (2019) 267.
120. C. Feng, C. Zhang, J. Guo, G. Li, B. Ye and L. Zou, *Anal. Chim. Acta*, 1176 (2021) 338781.
121. C. Feng, C. Zhang, J. Guo, G. Li, B. Ye and L. Zou, *Anal. Chim. Acta*, 1158 (2021) 338413.
122. R. M. Torrente-Rodriguez, S. Campuzano, V. R. Montiel, J. J. Montoya and J. M. Pingarron, *Biosens. Bioelectron.*, 86 (2016) 516.
123. Y. Yuan, G. Liu, Y. Chai and R. Yuan, *Sens. Actuat. B: Chem.*, 246 (2017) 402.
124. N. Xia, Z. Sun, F. Ding, Y. Wang, W. Sun and L. Liu, *ACS Sens.*, 6 (2021) 1166.
125. L. Liu, D. Deng, D. Wu, W. Hou, L. Wang, N. Li and Z. Sun, *Anal. Chim. Acta*, 1149 (2021) 338199.
126. N. Xia, T. Sun, L. Liu, L. Tian and Z. Sun, *Talanta*, 237 (2022) 122949.
127. L. Zhu, L. Yu and X. Yang, *ACS Appl. Mater. Interfaces*, 13 (2021) 42250.
128. H. Wang, C. Yang, H. Tang and Y. Li, *Anal. Chem.*, 93 (2021) 4593.
129. T. Hou, W. Li, X. Liu and F. Li, *Anal. Chem.*, 87 (2015) 11368-11374.
130. X. Liao, C. Zhang, J. O. Machuki, X. Wen, D. Chen, Q. Tang and F. Gao, *Talanta*, 226 (2021) 122058.
131. S. Li, H. Li, X. Li, M. Zhu, H. Li and F. Xia, *Anal. Chem.*, 93 (2021) 8354.
132. L. Li, Y. Zhang, S. Ge, L. Zhang, K. Cui, P. Zhao, M. Yan and J. Yu, *Anal. Chem.*, 91 (2019) 10273.
133. X. Liu, Z. Yan, Y. Sun, J. Ren and X. Qu, *Chem. Commun.*, 53 (2017) 6215.
134. D. Yang, Q. Mei, Y. Tang and P. Miao, *Electrochem. Commun.*, 103 (2019) 37.
135. D. Liu, S. Meng, X. Shen, Y. Li, X. Yan and T. You, *Sens. Actuat. B: Chem.*, 332 (2021) 129529.
136. Y. H. Yuan, B. Z. Chi, S. H. Wen, R. P. Liang, Z. M. Li and J. D. Qiu, *Biosens. Bioelectron.*, 102 (2018) 211.
137. L. Yang, X. Yin, B. An and F. Li, *Anal. Chem.*, 93 (2021) 1709.